

Stationary covariance spectra of discrete-time non-normal random recurrent dynamics

Jacob A. Zavatone-Veth*

Center for Brain Science, Harvard University, Cambridge, MA, USA and
Society of Fellows, Harvard University, Cambridge, MA, USA

(Dated: July 1, 2026)

Principal component analysis is widely used to characterize structure in the dynamics of recurrent neural networks. For stationary noise-driven dynamics, the distribution of variance among the principal components is determined by the spectrum of the stationary covariance matrix. While the spectral properties of this matrix are well-understood for linear networks with normal synaptic weight matrices, our understanding of the stationary covariance spectrum for random non-normal dynamics remains incomplete. In this note, we use a free-probability approach to formally derive a closed functional equation for the moment generating function of the limiting stationary covariance spectrum of discrete-time dynamics with random non-normal Gaussian weights. This characterization allows us to analyze the behavior of tail eigenvalues in the critical regime. In contrast, applying the same approach to the analogous continuous-time dynamics leads to an infinite hierarchy of Schwinger-Dyson equations, rather than a closed scalar equation. We conclude with some comments regarding the relevance of these results to comparisons of models of non-normal dynamics to neural data.

I. INTRODUCTION

Consider a noise-driven linear recurrent neural network, with N neurons that are connected through a weight matrix J . There are two classes of such dynamics which one might naturally consider: the discrete-time evolution

$$\mathbf{x}_{t+1} = \mathbf{J}\mathbf{x}_t + \mathbf{z}_t, \quad (1)$$

where $\mathbf{z}_t \sim \mathcal{N}(0, I_N)$, and the continuous-time evolution

$$\frac{d}{dt}\mathbf{x}(t) = -\mathbf{x}(t) + \mathbf{J}\mathbf{x}(t) + \mathbf{z}(t), \quad (2)$$

where now $\mathbf{z}(t)$ is white Gaussian noise. If \mathbf{J} has i.i.d. Gaussian elements $J_{ij} \sim \mathcal{N}(0, g/N)$ for a gain parameter $g > 0$ ¹—that is, it is a real Ginibre matrix—then (1) and (2) constitute minimal models for non-normal recurrent dynamics in discrete or continuous time, respectively; they are the linearized equivalents of the canonical model of random recurrent dynamics [1–9].

As \mathbf{J} is stable with high probability at large N provided that the gain parameter $g < 1$, the distribution of activity under either discrete- or continuous-time dynamics will relax to a Gaussian stationary distribution [10]. In discrete time, the stationary covariance $\Sigma_d = \lim_{t \rightarrow \infty} \mathbb{E}[\mathbf{x}_t \mathbf{x}_t^\top]$ solves the discrete Lyapunov equation

$$\Sigma_d = \mathbf{I}_N + \mathbf{J}\Sigma_d\mathbf{J}^\top, \quad (3)$$

and can be written as an infinite series:

$$\Sigma_d = \sum_{k=0}^{\infty} \mathbf{J}^k (\mathbf{J}^\top)^k. \quad (4)$$

In continuous time, the stationary covariance $\Sigma_c = \lim_{t \rightarrow \infty} \mathbb{E}[\mathbf{x}(t)\mathbf{x}(t)^\top]$ solves the continuous Lyapunov equation

$$(\mathbf{I}_N - \mathbf{J})\Sigma_c + \Sigma_c(\mathbf{I}_N - \mathbf{J})^\top = \mathbf{I}_N, \quad (5)$$

and can be written explicitly as

$$\Sigma_c = \int_0^{\infty} e^{\mathbf{J}t} e^{\mathbf{J}^\top t} e^{-2t} dt. \quad (6)$$

In either case, determining the eigenvalue spectrum of the stationary covariance is of interest because it determines the distribution of variance among the principal components of the stationary activity [2, 5]. This makes these simple random linear dynamical models important null models for analyses of recurrent neural computations based on principal component analysis [2, 5, 8, 11–13]. Alternatively, from a control theory perspective, the stationary covariance matrices Σ_d and Σ_c coincide with the discrete and continuous controllability Gramians, respectively. Then, the spectra are of interest because the eigenvalues determine the control costs along different dimensions [14]. Yet a third motivation for studying these dynamics comes from non-equilibrium statistical mechanics, where Ornstein-Uhlenbeck processes of the form (2) with non-normal interaction matrices give a canonical, minimal example of a non-equilibrium steady state [15–17].

In the case where the matrix \mathbf{J} is normal, the spectra of Σ_d and Σ_c are relatively straightforward to characterize because in that case \mathbf{J} admits an orthogonal eigen-decomposition [2, 14, 17]. However, for non-normal \mathbf{J} like the Ginibre matrices of interest, the eigenvectors are not orthonormal, and the spectra of Σ_d and Σ_c

* jzavatoneveth@fas.harvard.edu

¹ Our convention is that the *variance* of the elements of $\sqrt{N}\mathbf{J}$ is g . We note that it is standard in the neuroscience literature to use g instead for the standard deviation, and thus g^2 for the variance [1–3]. Because the variance appears much more frequently in our computations, directly denoting it by g lightens the notation.

are correspondingly harder to analyze as they are dependent on the eigenvector overlaps. While previous works have computed the asymptotic spectral distributions for related covariance matrices in other random-network or Ornstein-Uhlenbeck settings [14, 17], and considered the spectra of related covariance matrices for Ginibre \mathbf{J} [2, 8, 18],² an exact characterization in the present discrete-time quenched Ginibre setting is thus far lacking. Having such a characterization would be particularly desirable in light of recent work that seeks to compare the spectra of such models to neural data [11].

The primary purpose of this note is to record the fact that the bulk spectrum of eigenvalues of Σ_d can be characterized quite precisely in the limit $N \rightarrow \infty$. In particular, if we define the moment generating function

$$F_d(z) = \sum_{n=0}^{\infty} m_n z^n = \lim_{N \rightarrow \infty} \mathbb{E} \frac{1}{N} \text{tr}[(\mathbf{I}_N - z \Sigma_d)^{-1}], \quad (7)$$

where

$$m_n = \lim_{N \rightarrow \infty} \mathbb{E} \frac{1}{N} \text{tr}(\Sigma_d^n), \quad (8)$$

we find that $F_d(z)$ satisfies the functional equation

$$(1 - z)F_d(z) = F_d(gzF_d(z)) \quad (9)$$

subject to the condition $F_d(0) = 1$. Here, all expectations implicitly condition on the event that \mathbf{J} is stable. To our knowledge, this exact characterization of Σ_d has not been previously reported in the literature. We formally derive this result using free probability techniques in Section II. From a random matrix theory perspective, because Σ_d is the solution to a Lyapunov equation with quenched randomness \mathbf{J} , it is not a standard Wishart- or free-convolution-type object. Nonetheless, we obtain a closed functional equation thanks to the gauge symmetry of the limiting circular element. In contrast, applying an analogous approach in the continuous-time setting yields an infinite hierarchy of equations rather than a closed scalar equation for the corresponding spectral generating function; we will return to this in Section IV and the Discussion.

The functional equation (9) can also be written as a recurrence relation for the moments m_n , which shows that the condition $F_d(0) = 1$ selects a unique analytic solution. To do so, we start from the expansion $F_d(z) = \sum_{n=0}^{\infty} m_n z^n$, where we know that $m_0 = 1$. Using this expansion, we can re-write (9) as

$$\sum_{n=1}^{\infty} (m_n - m_{n-1}) z^n = \sum_{n=1}^{\infty} \left[\sum_{k=1}^n m_k g^k a_{n-k}^{(k)} \right] z^n, \quad (10)$$

where we have used the r -fold Cauchy convolution formula to write $F_d(z)^r = \sum_{k=0}^{\infty} a_k^{(r)} z^k$ for

$$a_k^{(r)} = \sum_{\substack{0 \leq j_1, \dots, j_r \leq k \\ j_1 + \dots + j_r = k}} m_{j_1} \cdots m_{j_r}. \quad (11)$$

Equating the coefficients of z^n for $n \geq 1$ on both sides, we find that

$$(1 - g^n) m_n = m_{n-1} + \sum_{k=1}^{n-1} g^k m_k a_{n-k}^{(k)}. \quad (12)$$

For any $0 < g < 1$, this is a forward recurrence that uniquely determines m_n in terms of the lower moments m_0, \dots, m_{n-1} . This proves uniqueness of the formal power series solution to (9), and also gives us an algorithmic procedure to compute the moments. For instance, $m_1 = (1 - g)^{-1}$, and $m_2 = (1 - g)^{-3} (1 + g)^{-1}$, which allows us to compute the normalized participation ratio of the spectrum:

$$\lim_{N \rightarrow \infty} \frac{1}{N} \frac{\text{tr}(\Sigma_d^2)}{\text{tr}(\Sigma_d^2)} = \frac{m_1^2}{m_2} = 1 - g^2. \quad (13)$$

Given a solution to (9), we can recover the spectral distribution using the fact that the Stieltjes transform $G(s)$ of the eigenvalue density is

$$G(s) = \frac{1}{s} F_d\left(\frac{1}{s}\right); \quad (14)$$

the density follows upon Stieltjes inversion:

$$\rho(\lambda) = \lim_{\epsilon \downarrow 0} \frac{1}{\pi} \text{Im} G(\lambda - i\epsilon). \quad (15)$$

As shown in Section III, the resulting density is compactly-supported, with a hard lower edge at $\lambda_- = 1$, and a soft upper edge determined by the solution to an implicit equation. In the critical limit $g \uparrow 1$, we show in Section III that $\lambda_+ \sim 2/(1 - g)^2$, and extract the density of eigenvalues in the tail. Away from the critical limit, we can solve the functional equation numerically, which produces an excellent match to numerical computation of the empirical spectral distribution (Figure 1). More quantitatively, we find that the first eight moments predicted by this result agree well with numerical estimation of empirical moments (see Figure 3 in Appendix B).

II. DERIVATION OF THE DISCRETE-TIME FUNCTIONAL EQUATION

A compact derivation of the claimed functional equation (9) for F_d is possible using free probability. We recall the basic ingredients required here; our treatment will be in general quite informal, and we refer the reader to the textbook of Mingo and Speicher [19] or a review article by Guionnet [20] for details. Free probability deals with

² See the discussion of Hu and Sompolinsky [2] in Section IV and Appendix A.

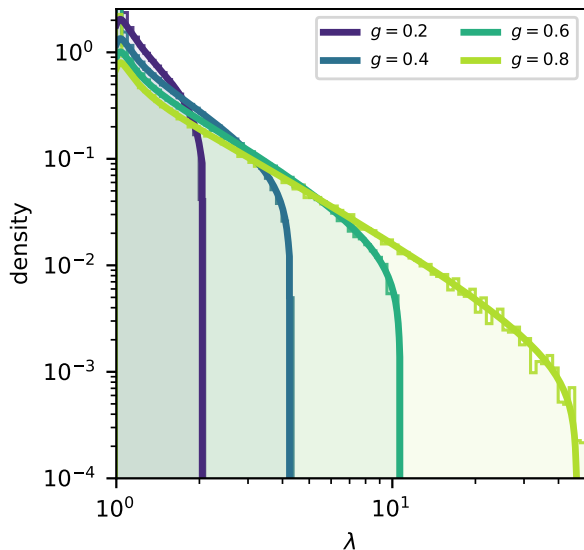


FIG. 1. Comparison of the density of eigenvalues of Σ_d predicted by numerical solution of the functional equation (9) and numerical eigendecomposition of Σ_d computed from a single realization of the random matrix \mathbf{J} with $N = 2048$. Solid lines show theory, and shaded stair-step patches show empirical histograms estimated by binning. Different colors show different values of the gain parameter g . See Appendix B for details of the numerical scheme used to approximately solve (9).

an algebra of random operators, equipped with a linear trace functional τ satisfying $\tau(1) = 1$ for 1 the identity element, which defines expectations. We will formally argue below that the empirical spectral distribution of Σ_d converges to the spectral distribution of a free random variable σ_d defined by the formal power series

$$\sigma_d = \sum_{k=0}^{\infty} c^k (c^*)^k, \quad (16)$$

where c is a circular element satisfying $\tau(cc^*) = g$. This follows from one of the most fundamental results from free probability: that spectral properties of real matrices with i.i.d. Gaussian elements in the limit $N \rightarrow \infty$ are captured by circular elements, with \mathbf{J} being asymptotically replaced by c and \mathbf{J}^\top being replaced by c^* [19, 21].

We will use two important properties of circular elements in our derivation. First, circular elements have a gauge symmetry: their distribution is invariant under multiplication by complex numbers of modulus 1, *i.e.*, $e^{i\phi}c$ and c have the same distribution for any real ϕ . This gauge symmetry emerges asymptotically from the symmetries of the finite-size ensemble. Second, circular elements admit an equivalent of Gaussian integration by parts known as “free differencing”: for some operator P we have

$$\tau(cP) = g(\tau \otimes \tau)\partial_{c^*}P, \quad (17)$$

where ∂_{c^*} is a derivation satisfying $\partial_{c^*}c = 0$, $\partial_{c^*}c^* =$

$1 \otimes 1$, and also the Leibniz rule

$$\partial_{c^*}(UV) = (\partial_{c^*}U)(1 \otimes V) + (U \otimes 1)(\partial_{c^*}V). \quad (18)$$

These facts are sufficient to derive the claimed functional equation.

To start, we first note that the formal power series $\sigma_d = \sum_{k=0}^{\infty} c^k (c^*)^k$ defines a bounded operator. To see this, note that the spectral radius of the circular element c is $\sqrt{g} < 1$, so $\lim_{k \rightarrow \infty} \|c^k\|^{1/k} = \sqrt{g}$. Thus, if we choose any $\sqrt{g} < \rho < 1$, for all sufficiently large k we have $\|c^k\| \leq \rho^k$, which in turn implies that $\|c^k (c^*)^k\| = \|c^k\|^2 \leq \rho^{2k}$, which is summable because $\rho < 1$. Thus, σ_d is a bounded positive operator. Then, noting that

$$m_n = \tau(\sigma_d^n), \quad (19)$$

the series expansion for $F_d(z)$ converges in an open disk $|z| < 1/\|\sigma_d\|$, and moreover is analytic in that disk. Summing the operator-level series, we can write

$$F_d(z) = \tau(R(z)), \quad \text{where } R(z) = (1 - z\sigma_d)^{-1}. \quad (20)$$

We now note that the series expansion for σ_d means that it satisfies an operator-level Lyapunov equation

$$\sigma_d = 1 + c\sigma_d c^*. \quad (21)$$

We use this to expand $\sigma_d R$ in two different ways. First, the Lyapunov equation directly implies that

$$\tau(\sigma_d R) = F_d(z) + \tau(c\sigma_d c^* R). \quad (22)$$

Second, for any $z \neq 0$ we have the algebraic identity

$$\tau(\sigma_d R) = \frac{F_d(z) - 1}{z}, \quad (23)$$

which follows from the fact that

$$R - 1 = (1 - z\sigma_d)^{-1}[1 - (1 - z\sigma_d)] = z\sigma_d R. \quad (24)$$

Combining these two identities, we find that

$$(1 - z)F_d(z) - 1 = z\tau(c\sigma_d c^* R). \quad (25)$$

Now, consider

$$\mu_n = \tau(c\sigma_d^n c^* R), \quad (26)$$

such that the term we need to compute is μ_1 . Using the integration by parts identity and the Leibniz rule,

$$\begin{aligned} \mu_n &= g(\tau \otimes \tau)[(\partial_{c^*}\sigma_d^n)(1 \otimes c^* R)] \\ &\quad + g(\tau \otimes \tau)[(\sigma_d^n \otimes R)] \\ &\quad + g(\tau \otimes \tau)[(\sigma_d^n c^* \otimes 1)\partial_{c^*}R]. \end{aligned} \quad (27)$$

We consider each of these three terms in turn. First, using the formula $\sigma_d = 1 + c\sigma_d c^*$, we find that $\partial_{c^*}\sigma_d$ satisfies

$$\partial_{c^*}\sigma_d = (c \otimes 1)\partial_{c^*}\sigma_d(1 \otimes c^*) + c\sigma_d \otimes 1, \quad (28)$$

which upon iteration leads to the series expansion

$$\partial_{c^*} \sigma_d = \sum_{k=0}^{\infty} c^{k+1} \sigma_d \otimes (c^*)^k. \quad (29)$$

Repeated application of the Leibniz rule then leads to

$$\partial_{c^*} \sigma_d^n = \sum_{k=0}^{\infty} \sum_{\ell=0}^{n-1} (\sigma_d^\ell c^{k+1} \sigma_d) \otimes ((c^*)^k \sigma_d^{n-1-\ell}). \quad (30)$$

Moreover, differentiating the operator inverse yields

$$\partial_{c^*} R = z(R \otimes 1) \partial_{c^*} \sigma_d (1 \otimes R), \quad (31)$$

which gives the explicit expansion

$$\partial_{c^*} R = z \sum_{k=0}^{\infty} (R c^{k+1} \sigma_d) \otimes ((c^*)^k R). \quad (32)$$

Thus, the first term in μ_n is

$$\begin{aligned} & (\tau \otimes \tau)[(\partial_{c^*} \sigma_d^n)(1 \otimes c^* R)] \\ &= \sum_{k=0}^{\infty} \sum_{\ell=0}^{n-1} \tau(\sigma_d^\ell c^{k+1} \sigma_d) \tau((c^*)^k \sigma_d^{n-1-\ell} c^* R). \end{aligned} \quad (33)$$

But, we note that the two traces inside the sum are not invariant under $c \mapsto e^{i\phi} c$, as they carry different numbers of powers of c and c^* . This holds because σ_d and thus R carry balanced pairings of c and c^* , hence there is nothing to counteract the extra power of c in the left factor. Therefore, each trace must vanish, and thus

$$(\tau \otimes \tau)[(\partial_{c^*} \sigma_d^n)(1 \otimes c^* R)] = 0. \quad (34)$$

The second term is simply

$$(\tau \otimes \tau)[\sigma_d^n \otimes R] = \tau(\sigma_d^n) \tau(R) = m_n F_d(z). \quad (35)$$

The third term is

$$\begin{aligned} & (\tau \otimes \tau)[(\sigma_d^n c^* \otimes 1) \partial_{c^*} R] \\ &= z \sum_{k=0}^{\infty} \tau[\sigma_d^n c^* R c^{k+1} \sigma_d] \tau[(c^*)^k R]. \end{aligned} \quad (36)$$

As we encountered in the first term, for any $k > 0$ we must have $\tau[(c^*)^k R] = 0$ because $(c^*)^k R$ is not invariant under $c \mapsto e^{i\phi} c$. This leaves us with the $k = 0$ term:

$$(\tau \otimes \tau)[(\sigma_d^n c^* \otimes 1) \partial_{c^*} R] = z \tau[\sigma_d^n c^* R c \sigma_d] \tau[R] \quad (37)$$

$$= z \tau[c \sigma_d^{n+1} c^* R] F_d(z) \quad (38)$$

$$= z \mu_{n+1} F_d(z), \quad (39)$$

where we have used the fact that τ is cyclic.

Putting these results together, we conclude that

$$\mu_n = g m_n F_d(z) + g z \mu_{n+1} F_d(z). \quad (40)$$

Iterating this recursion, we find that

$$\mu_1 = \frac{1}{z} \sum_{n=1}^{\infty} m_n (g z F_d(z))^n = \frac{F_d(g z F_d(z)) - 1}{z}, \quad (41)$$

where we recognize the definition of F_d . This iteration is justified for z sufficiently small; we can then extend by analyticity to all z in the domain where F_d is analytic. Therefore,

$$(1 - z) F_d(z) - 1 = z \mu_1 = F_d(g z F_d(z)) - 1, \quad (42)$$

hence we conclude that, as claimed,

$$(1 - z) F_d(z) = F_d(g z F_d(z)). \quad (43)$$

We now remark on a mathematical issue which we have so far swept under the rug: the claim of convergence of the spectrum of Σ_d to that of σ_d . As elsewhere, we define convergence of spectral distributions in the sense that the normalized trace moments of Σ_d converge in expectation to those of σ_d , conditioned on the event that \mathbf{J} is stable (an event whose probability tends to one as $N \rightarrow \infty$). This is not necessarily obvious, because the standard free probability result is that non-commutative *polynomials* in \mathbf{J} converge to the corresponding polynomials in c as $N \rightarrow \infty$ [19]. However, we can justify this formally, up to a uniform convergence assumption which we do not prove here, by writing Σ_d in an integral form. Assuming \mathbf{J} is stable, we can define

$$\mathbf{H}(\theta) = (\mathbf{I}_N - e^{i\theta} \mathbf{J})^{-1} = \sum_{k=0}^{\infty} e^{ik\theta} \mathbf{J}^k \quad (44)$$

for an angle $\theta \in [0, 2\pi)$. Then, using Plancherel's theorem applied to Fourier series,

$$\int_0^{2\pi} \mathbf{H}(\theta) \mathbf{H}(\theta)^* \frac{d\theta}{2\pi} = \sum_{k=0}^{\infty} \mathbf{J}^k (\mathbf{J}^\top)^k = \Sigma_d. \quad (45)$$

Therefore, for stable \mathbf{J} , we have

$$\Sigma_d = \int_0^{2\pi} (\mathbf{I}_N - e^{i\theta} \mathbf{J})^{-1} (\mathbf{I}_N - e^{-i\theta} \mathbf{J}^\top)^{-1} \frac{d\theta}{2\pi}. \quad (46)$$

We claim that we can use this expression to argue that the limiting spectral distribution of Σ_d tends to that of

$$\sigma_d = \int_0^{2\pi} (1 - e^{i\theta} c)^{-1} (1 - e^{-i\theta} c^*)^{-1} \frac{d\theta}{2\pi}. \quad (47)$$

Before doing so, we show that this definition coincides with how we defined σ_d before. This can be seen from applying in reverse the same argument as we used to obtain the integral formula for Σ_d : Plancherel's theorem implies that we have the convergent expansion

$$\int_0^{2\pi} (1 - e^{i\theta} c)^{-1} (1 - e^{-i\theta} c^*)^{-1} \frac{d\theta}{2\pi} = \sum_{k=0}^{\infty} c^k (c^*)^k, \quad (48)$$

which is the desired result.

Now, we argue that these integral expressions allow us to identify (47) as giving the limiting spectral distribution of (46). For each fixed θ , the integrand in (46) is a non-commutative self-adjoint rational function of \mathbf{J} . Then, using the invertibility of $1 - e^{i\theta}\mathbf{J}$ and $1 - e^{i\theta}c$ along with the standard spectral distribution convergence of real Ginibre matrices to circular elements, we can apply Proposition 28 of Collins *et al.* [22] to conclude that the empirical spectral distribution of the integrand in (46) tends to the limit of the corresponding integrand in (47).

To pass from this pointwise-in- θ statement to full spectral distribution convergence, we would need to control convergence uniformly enough to show that the traces of powers of Σ_d converge to those of σ_d (*i.e.*, of n -fold integrals of this form), and careful handling of the rate at which the probability \mathbf{J} is unstable tends to zero. Alternatively, we could infinitesimally regularize the resolvents by shifting \mathbf{I}_N to $(1 + \eta)\mathbf{I}_N$ for a small parameter η which we let tend to zero after taking $N \rightarrow \infty$. Either way, we do not expect these technical considerations to alter the limiting spectral distribution. Thus, subject to the assumption of uniform convergence, this identifies the limiting spectral density obtained above.

III. SPECTRAL EDGES AND CRITICAL LIMITS IN DISCRETE TIME

We now turn our attention to a few properties of the limiting spectral density of Σ_d that we can extract from the functional equation (9). First, we consider the edges of the spectrum. As σ_d is a bounded operator, we know that the spectrum is compactly-supported; we will show that it has a lower edge at 1 and an upper edge at some finite λ_+ determined by the solution to an implicit equation. Using the Stieltjes transform relationship $G(s) = F_d(1/s)/s$, we can re-write the functional equation as $(s - 1)w = gF_d(w)$ upon letting $w = gG(s)$. Formally, we can then write the solution for the inverse transform as

$$s = K(w(s)), \quad \text{for} \quad K(w) = 1 + \frac{g}{w}F_d(w). \quad (49)$$

We can determine the spectral edges, at least implicitly, by studying the properties of this equation [19]. In particular, the spectral edges can be determined by examining when solution branches that would correspond to s outside of the support of the spectrum terminate, which is made easier by the fact that $w = gG(s)$ is real for real s outside of the spectral support.

The minimum eigenvalue λ_- clearly must be at least 1, as the Lyapunov equation $\sigma_d = 1 + c\sigma_d c^*$ implies that $\sigma_d \succeq 1$. The question is then whether λ_- is always pinned to this lower bound. For s below the spectral support of σ_d , we have $G(s) = \tau((s - \sigma_d)^{-1}) < 0$ and thus $w < 0$.

Moreover, as $F_d(z) = \tau((1 - z\sigma_d)^{-1})$, we see that

$$\frac{w^2}{g}K'(w) = wF_d'(w) - F_d(w) = \tau\left(\frac{2\sigma_d w - 1}{(1 - w\sigma_d)^2}\right). \quad (50)$$

As $\sigma_d \succeq 1$, this implies that $K'(w) < 0$ for all $w < 0$. Moreover, we see that $K(w) \rightarrow 1$ as $w \rightarrow -\infty$, because $F_d(w) \sim \tau(\sigma_d^{-1})/|w|$ as $w \rightarrow -\infty$. This means that the solution branch does not terminate at a finite value of w , as would be required to give a soft edge above 1, and thus we always have $\lambda_- = 1$.

Now we consider the maximum eigenvalue λ_+ . For s above the spectral support of σ_d , $G(s) > 0$, and moreover we have $G(s) \sim 1/s \rightarrow 0$ as $s \rightarrow \infty$. This means that the equation should have an upper branch starting from $w = 0$ (where $K(w) \rightarrow \infty$), with w increasing as s approaches the upper edge of the spectrum. The question is then whether $K'(w)$ can vanish for some finite w_+ . From (50), we see that this is indeed possible, as for $w > 0$ the numerator of the trace can vanish. Under the usual regular-edge assumption for the physical branch of the inverse Stieltjes transform [19], the upper edge is obtained from the smallest solution $w_+ > 0$ to the equation

$$w_+ F_d'(w_+) = F_d(w_+). \quad (51)$$

Given a solution for w_+ , we then identify the upper edge of the spectrum as

$$\lambda_+ = K(w_+) = 1 + \frac{g}{w_+}F_d(w_+). \quad (52)$$

Unlike the lower edge, this is a soft edge. We see in Figure 1 that numerically solving for λ_+ produces good agreement with simulations.

We now turn our attention to the critical limit $g \uparrow 1$, where the dynamics are nearly unstable. Concretely, we suppose that we first take $N \rightarrow \infty$ at fixed $g < 1$, and then take $g \uparrow 1$. Here, we can expand the functional equation to obtain an approximate solution for the long tail of large eigenvalues. Let $\delta = 1 - g$, such that the critical limit is $\delta \downarrow 0$. As we expect the largest eigenvalue to diverge as $\delta \downarrow 0$, we expand F_d in a small neighborhood around $z = 0$, as the branch point at $z = 1/\lambda_+$ approaches the origin. We therefore make a scaling *Ansatz*

$$z = \delta^2 \zeta, \quad F_d(z) = 1 + \delta f(\zeta) + \mathcal{O}(\delta^2). \quad (53)$$

Expanding both sides of the functional equation (9) under this *Ansatz*, we have

$$\begin{aligned} 1 + \delta f(\zeta) - \delta^2 \zeta + \mathcal{O}(\delta^3) \\ = 1 + \delta f(\zeta) + \delta^2 f'(\zeta)(f(\zeta) - 1)\zeta + \mathcal{O}(\delta^3), \end{aligned} \quad (54)$$

so we conclude that $f(\zeta)$ solves

$$-1 = f'(\zeta)(f(\zeta) - 1). \quad (55)$$

This justifies our scaling *Ansatz*; other choices would lead to trivial scaling at leading order in δ . From the fact that

$F_d(z=0) = 1$, we have the initial condition $f(\zeta=0) = 0$. Then, we can solve for

$$f(\zeta) = 1 - \sqrt{1 - 2\zeta}. \quad (56)$$

This branch ceases to be real at $\zeta_+ = 1/2$, hence we conclude that as $\delta \downarrow 0$ we have

$$\lambda_+ \sim \frac{1}{\delta^2 \zeta_+} = \frac{2}{\delta^2}. \quad (57)$$

We therefore consider the tail density of eigenvalues on the critical scale

$$\lambda = \frac{x}{\delta^2} \quad (58)$$

for $0 < x < 2$. Writing the infinitesimal quantity appearing in the Stieltjes inversion formula as $i0$, we have

$$G\left(\frac{x}{\delta^2} - i0\right) = \frac{\delta^2}{x} \left[1 + \delta f\left(\frac{1}{x} + i0\right) + \mathcal{O}(\delta^2) \right]. \quad (59)$$

Continuing the same branch for $f(\zeta)$ into the region $\zeta > 1/2$, we see that it connects to a branch with positive imaginary part:

$$f\left(\frac{1}{x} + i0\right) = 1 + i\sqrt{\frac{2}{x} - 1}. \quad (60)$$

Then, we find that

$$\text{Im } G\left(\frac{x}{\delta^2} - i0\right) = \frac{\delta^3}{x} \sqrt{\frac{2}{x} - 1} + \mathcal{O}(\delta^4), \quad (61)$$

which gives the tail density

$$\frac{1}{\delta^2} \rho\left(\frac{x}{\delta^2}\right) \sim \delta \frac{\sqrt{x(2-x)}}{\pi x^2} \quad (62)$$

for $0 < x < 2$. Thus, near the soft upper edge of the critical tail, the tail density vanishes as $\sqrt{2-x}$.

This allows us to estimate the scaling of eigenvalues in the tail. Using the tail density, we can estimate the count of eigenvalues above some level x/δ^2 by

$$\mathbb{P}\left[\lambda > \frac{x}{\delta^2}\right] \sim \delta \int_x^2 \frac{\sqrt{u(2-u)}}{\pi u^2} du \quad (63)$$

$$= \frac{2\delta}{\pi} \left[\sqrt{\frac{2-x}{x}} - \arccos \sqrt{\frac{x}{2}} \right]. \quad (64)$$

Away from the upper extreme of the tail, we can estimate the scaling by expanding near $x=0$, which gives

$$\mathbb{P}\left[\lambda > \frac{x}{\delta^2}\right] \sim \delta \frac{2\sqrt{2}}{\pi\sqrt{x}} \quad (65)$$

for $\delta^2 \ll x \ll 1$. Thus, if λ_k is the k -th largest among N eigenvalues, for $N\delta \ll k \ll N$ we expect that

$$\lambda_k \sim \frac{8}{\pi^2} \left(\frac{N}{k}\right)^2. \quad (66)$$

In Figure 2, we validate these predictions in two ways. First, we show that the ranked eigenvalues collapse almost perfectly onto the curve predicted by (64). In particular, if we define the normalized rank $\kappa = k/N\delta$, (64) is of the form $\kappa = R(x)$, which gives us a theoretical prediction for the eigenvalue as a function of rank. Second, we show that the simple inverse-squared scaling of eigenvalue with normalized rank gives good predictions for the scaling in an intermediate regime, with corrections visible for the largest and smallest eigenvalues. This is consistent with the expectation that the scaling should hold for $N\delta \ll k \ll N$.

IV. CONTINUOUS-TIME DYNAMICS AND THE LOSS OF SCALAR CLOSURE

Now, we show why it is harder to analyze the limiting spectrum of Σ_c . What we will find is that expanding the definition of the moment generating function for Σ_c leads to an infinite hierarchy of Schwinger-Dyson equations, rather than a closed scalar equation for the generating function itself. This difference reflects the fact that σ_d is gauge-neutral as a function of c and c^* —each term is invariant under $c \mapsto e^{i\theta}c$ —while σ_c is not.

Before embarking on the analysis, we note that the stationary covariance Σ_c considered here is distinct from the frequency-domain covariance $\mathbf{Q}(\omega)$ studied by Hu and Sompolinsky [2]. This object is obtained by taking the Fourier transform of the stationary time-lagged covariance $\mathbf{Q}(\tau) = \lim_{t \rightarrow \infty} \mathbb{E}[x(t)x(t+\tau)^\top]$, and is given for a linear network by

$$\mathbf{Q}(\omega) = [(1+i\omega)\mathbf{I}_N - \mathbf{J}]^{-1}[(1-i\omega)\mathbf{I}_N - \mathbf{J}^\top]^{-1}. \quad (67)$$

To relate $\mathbf{Q}(\omega)$ to Σ_c , we apply Plancherel's theorem to the matrix-valued function $\Theta(t)e^{-(I-\mathbf{J})t}$ [10], which gives

$$\Sigma_c = \int_{-\infty}^{\infty} \mathbf{Q}(\omega) \frac{d\omega}{2\pi}. \quad (68)$$

As \mathbf{J} is non-normal, the eigenvectors of $\mathbf{Q}(\omega)$ are ω -dependent, meaning that the spectral density of $\mathbf{Q}(\omega)$ does not directly determine that of Σ_c [7]. Thus, while Hu and Sompolinsky [2] obtained an interpretable expression for the spectral density of $\mathbf{Q}(\omega)$, we do not obtain a similarly-compact characterization of the spectrum of Σ_c . We will return to this distinction in Appendix A, where we give a compact derivation of the Hu-Sompolinsky density.

Returning to Σ_c , the relevant free random variable is

$$\sigma_c = \int_0^\infty e^{ct} e^{c^*t} e^{-2t} dt, \quad (69)$$

which satisfies

$$\sigma_c = \frac{1}{2} + \frac{1}{2}(c\sigma_c + \sigma_c c^*). \quad (70)$$

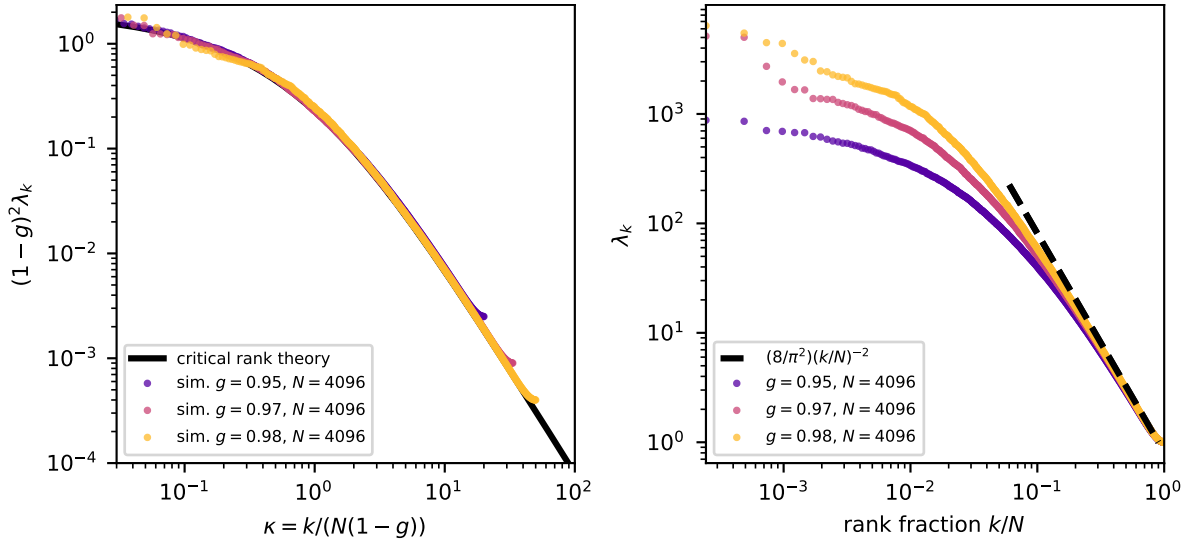


FIG. 2. Scaling of eigenvalues in the critical tail. *Left*: Collapse of scaled tail eigenvalues $(1-g)^2 \lambda_k$ as a function of normalized rank $\kappa = k/(N(1-g))$ across different values of g . *Right*: In the intermediate-rank regime, the eigenvalues decay with rank approximately according to the predicted scaling law with exponent 2. As these simulations are done near the stability threshold $g = 1$, we numerically exclude realizations with $\rho(\mathbf{J}) > 1 - \varepsilon$ for a stability threshold $\varepsilon = 10^{-3}$. This ensures that the computation of the stationary covariance Σ_d is numerically stable.

As the spectral radius of c is bounded, the integral converges to a bounded operator. Formally, the fact that the limiting spectral distribution of Σ_c coincides with the spectral distribution of σ_c follows from using the Fourier representation (68), applying the rational-function convergence result of Collins *et al.* [22], and then passing back from frequency space to real space. Mirroring the discrete case, a fully rigorous justification would require uniform-in- ω control on the convergence of rational functions of \mathbf{J} to those of c .

By expanding the two exponentials and evaluating the integral over time, we obtain a formal series expansion

$$\sigma_c = \sum_{j,k=0}^{\infty} \alpha_{jk} c^j (c^*)^k, \quad (71)$$

where

$$\alpha_{jk} = \frac{1}{j!k!} \int_0^{\infty} t^{j+k} e^{-2t} dt = \frac{1}{2^{j+k+1}} \binom{j+k}{k}. \quad (72)$$

As in the series expansion for σ_d , this series defines a bounded operator thanks to the fact that, for any $\sqrt{g} < \rho < 1$, for all j and k large enough we have $\|c^j (c^*)^k\| \leq \rho^{j+k}$. However, because it contains terms with different powers of c and c^* , it is not invariant under $c \mapsto e^{i\phi} c$. This will turn out to be the source of the obstruction to obtaining scalar closure as we did in the discrete case. σ_d (and thus its resolvent) are neutral under gauge transformations $c \mapsto e^{i\phi} c$, which means that traces of powers of c against the resolvent vanish by gauge symmetry. In contrast, σ_c is not gauge-neutral, so the analogous correlators are not forced to vanish by the gauge symmetry.

Now, we proceed with the analysis. Analogously to the discrete-time case, we let

$$F_c(z) = \tau(R(z)), \quad \text{where } R(z) = (1 - z\sigma_c)^{-1}. \quad (73)$$

Again, for any $z \neq 0$ we have the algebraic identity

$$\tau(\sigma_c R) = \frac{F_c(z) - 1}{z}; \quad (74)$$

what is different is that we now obtain the expansion

$$\tau(\sigma_c R) = \frac{1}{2} F_c(z) + \frac{1}{2} [\tau(c\sigma_c R) + \tau(\sigma_c c^* R)] \quad (75)$$

from the Lyapunov equation, where in the second line we have used the fact that R and σ_c commute. This leads to the equation

$$F_c(z) - 1 - \frac{1}{2} z F_c(z) = \frac{1}{2} z [\tau(c\sigma_c R) + \tau(\sigma_c c^* R)] \quad (76)$$

which, using the algebraic identity $z\sigma_c R = R - 1$ and the fact that $\tau(c) = \tau(c^*) = 0$, simplifies to

$$F_c(z) - 1 - \frac{1}{2} z F_c(z) = \frac{1}{2} [\tau(cR) + \tau(cR(z^*))^*], \quad (77)$$

where we use the fact that $\tau(c^* R) = \tau(cR(z^*))^*$.

We now integrate by parts:

$$\tau(cR) = g(\tau \otimes \tau) \partial_{c^*} R \quad (78)$$

$$= gz(\tau \otimes \tau) [(R \otimes 1) \partial_{c^*} \sigma_c (1 \otimes R)]. \quad (79)$$

To determine $\partial_{c^*} \sigma_c$, we can differentiate the Lyapunov equation to get

$$\partial_{c^*} \sigma_c = \frac{1}{2} (\sigma_c \otimes 1) + \frac{1}{2} (c \otimes 1) \partial_{c^*} \sigma_c + \frac{1}{2} \partial_{c^*} \sigma_c (1 \otimes c^*), \quad (80)$$

which on iteration leads to the series expansion

$$\partial_{c^*} \sigma_c = \sum_{j,k=0}^{\infty} \alpha_{jk} (c^j \sigma_c) \otimes (c^*)^k, \quad (81)$$

where α_{jk} is as in (72). Substituting this expansion into the formula for $\tau(cR)$, we have

$$\tau(cR) = gz \sum_{j,k=0}^{\infty} \alpha_{jk} \tau(Rc^j \sigma_c) \tau((c^*)^k R). \quad (82)$$

However, unlike in the discrete case, we cannot use distributional invariance under $c \mapsto e^{i\phi} c$ to argue that all but a few of the terms in this sum vanish, because σ_c itself contains both gauge-invariant and gauge-variant terms. This is evident from the series expansion (71).

Therefore, within this free-differencing approach, we do not obtain a simple closed equation for $F_c(z)$. Instead, we find that it is coupled to an infinite family of correlators like $\tau(c^k R)$ and $\tau(Rc^j \sigma_c)$. We could in principle write down an infinite set of coupled Schwinger-Dyson equations that together determine these objects—as the equations relating traces of these correlators are of Schwinger-Dyson type [20]. This would allow us to algorithmically compute statistics like moments of the spectral distribution—with the complexity of the computation increasing rapidly as we go to higher moments—but the simple scalar reduction is lost. We will therefore content ourselves with the fact that we have a clear picture for why the equation for the generating function does not close in the same simple way as it did in the discrete case.

V. DISCUSSION

We have formally shown that the stationary covariance spectrum of a discrete-time linear recurrent neural network with non-normal random weights satisfies a simple functional equation (9). This allows us to characterize the distribution of variance among principal components, and extract the long tail of eigenvalues in the critical regime $g \uparrow 1$ (Section III). In contrast, we found that applying the same free probability approach to the analogous continuous-time dynamics leads to an infinite hierarchy of Schwinger-Dyson equations, rather than a single scalar functional equation (Section IV). In continuous time, the frequency-domain covariance $\mathbf{Q}(\omega)$ (in particular its zero-frequency limit, which gives the long-time-window covariance) is comparatively simple to analyze; we give a compact proof of the density obtained by Hu and Sompolinsky [2] (Appendix A). We now comment on some of the implications of our results, and potential directions for future inquiry.

As we noted in Section IV, the distinction in complexity of the characterization of the spectral distribution in discrete and continuous time arises from a difference in the symmetries of the stationary covariances. Σ_d is a sum

of balanced terms $\mathbf{J}^k (\mathbf{J}^\top)^k$, which translate into gauge-invariant terms $c^k (c^*)^k$ at the free probability level. In contrast, Σ_c includes all balanced and imbalanced terms $\mathbf{J}^j (\mathbf{J}^\top)^k$, which leads to gauge-dependent terms $c^j (c^*)^k$ for $j \neq k$. The gauge-invariance in the discrete case enables us to show that all but a finite number of terms in the expansions we encounter vanish, leading to a closed equation for the generating function F_d , while no such reduction to a closed equation for F_c is immediately apparent in the continuum. This obstruction is consistent with the broader role of eigenvector non-orthogonality in non-normal Langevin dynamics, where stationary correlations, response functions, and entropy production depend explicitly on Chalker-Mehlig-type eigenvector overlaps [2, 7, 16, 23]. As our main focus is on the simplicity of the discrete-time result, we have not endeavored to perform a further detailed analysis of the continuous-time hierarchy. This will be an important and interesting topic for future work.

The Lyapunov equation $\sigma_d = 1 + c\sigma_d c^*$ resembles a class of fixed-point equations known as matrix or free *perpetuities*, which have very recently been studied in the random matrix literature [24, 25]. These equations take the form of distributional affine fixed-point equations $\mathbf{X} \stackrel{d}{=} \mathbf{A} + \mathbf{B}\mathbf{X}\mathbf{B}^\top$, where (\mathbf{A}, \mathbf{B}) is a pair of random matrices or free random variables. However, the solution \mathbf{X} to the perpetuity is assumed to be independent (or, in the limit, free) of the pair (\mathbf{A}, \mathbf{B}) . This is manifestly not true of the Lyapunov equation studied here, as σ_d is defined by the solution to the Lyapunov equation for a fixed realization of the circular element c . In other words, the randomness in the Lyapunov equation is quenched, while in some sense in a perpetuity it is annealed. With this distinction in mind, it would be interesting to connect the spectral laws for free perpetuities to those for the solutions to random Lyapunov equations.

We now return to the neuroscientific motivation of our study: the use of stationary, random linear recurrent dynamics as a null model for principal component spectra in richer recurrent models and in recordings of neural activity. In this regard, our work is substantially motivated by a recent paper of Pachitariu *et al.* [11], which compared the stationary covariance spectrum of continuous-time dynamics with varying choices of connectivity matrix ensemble to measurements of brainwide activity in mice. Based on simulations, Pachitariu *et al.* [11] conjectured that the critical tail of eigenvalues of Σ_c decays with rank with an exponent of 5/4. While we have not been able to prove this conjecture, we can show that the analogous discrete-time model has a yet larger ranked-eigenvalue exponent of 2. This is in further tension with their finding that neural recordings across several cortical and sub-cortical areas show decay exponents between 0.75 and 0.8, which are closer to, but do not coincide with, the 2/3 exponent predicted by taking \mathbf{J} to be a *symmetric* Gaussian random matrix. Our results thus underscore the fact that, even in null models, one can substantially change the statistics of critical dynamics

through seemingly-innocuous adjustments, like temporal discretization [12].

Finally, we note in closing that we have restricted our attention to linear recurrent dynamics. This enabled us to leverage the exact finite- N expressions available for the stationary covariance in the linear setting, which in turn allowed the direct application of free probability. However, nonlinear random recurrent neural networks would of course constitute a much richer class of null models for principal component analysis of stationary activity, as they can display true chaotic behavior [1]. In a pair of recent works, Clark [26] and Wakhloo [27] have shown that the long-time-window covariance of a nonlinear network with random weights can, in the $N \rightarrow \infty$ limit, be replaced by an effective linear network. This result proves a conjecture by Shen and Hu [18], who used a linearization of this form to extend the Hu and Sompolinsky [2] spectral density from linear to nonlinear networks. These equivalences are analogous to an ever-expanding array of so-called Gaussian equivalence theorems that have been proved for random feedforward neural networks [28, 29]. In light of the results we have obtained here, it would be interesting to extend these equivalences and the resulting spectral characterizations to the stationary setting.

ACKNOWLEDGEMENTS

The author thanks Blake Bordelon and David Clark for inspiring discussions and helpful comments. This work was supported by the Office of the Director of the NIH under Award Number DP5OD037354, and by a Junior Fellowship from the Harvard Society of Fellows.

The author used GPT 5.5 Pro to generate the initial version of the code used to make Figures 1 and 2, and to check the manuscript for typographical errors. He subsequently verified and edited the code, and takes responsibility for the content.

DATA AND CODE AVAILABILITY

Code to reproduce all figures is available on GitHub at <https://github.com/jzavatoneveth/discrete-nonnormal-dynamics-spectrum>. No external datasets were used; the figures depend only on the results of numerical simulations implemented in the code on GitHub.

Appendix A: A tractable question in continuous time: recovering the Hu-Sompolinsky density

As a counterpoint to the lack of scalar closure we found in Section IV for Σ_c , we now show that the free probability approach allows us to give a very compact derivation of Hu and Sompolinsky [2]’s result for the spectrum of

the frequency-domain covariance

$$\mathbf{Q}(\omega) = [(1 + i\omega)\mathbf{I}_N - \mathbf{J}]^{-1}[(1 - i\omega)\mathbf{I}_N - \mathbf{J}^\top]^{-1}. \quad (\text{A1})$$

For a non-zero complex number ζ such that $|\zeta| > \sqrt{g}$, define the operator

$$q(\zeta) = (\zeta - c)^{-1}(\zeta^* - c^*)^{-1}. \quad (\text{A2})$$

Then, as $N \rightarrow \infty$, the empirical spectral distribution of $\mathbf{Q}(\omega)$ tends to the spectral distribution of $q(1 + i\omega)$. As elsewhere, we define the moment generating function

$$F(z) = \tau(R(z)), \quad \text{for } R(z) = (1 - zq)^{-1}. \quad (\text{A3})$$

Our goal is, as in preceding sections, to obtain a closed functional equation for F .

Our approach will be to view q as the solution to the equation

$$(\zeta - c)q(\zeta^* - c^*) = 1, \quad (\text{A4})$$

and expand this equation in two ways. Defining the shifted circular element $a = \zeta - c$, we can write

$$aq = (a^*)^{-1} \quad \text{and} \quad qa^* = a^{-1}. \quad (\text{A5})$$

Tracing both equations against R and using the definition of a , this gives

$$\zeta M(z) - \tau(cqR) = \tau((a^*)^{-1}R), \quad (\text{A6})$$

$$\zeta^* M(z) - \tau(c^*qR) = \tau(a^{-1}R), \quad (\text{A7})$$

where we let $M(z) = \tau(qR) = \frac{1}{z}(F(z) - 1)$ for brevity. We now integrate by parts, using the fact that for c^* the relevant free difference is ∂_c . By differentiating the functional equation,

$$\partial_{c^*}q = q \otimes (a^*)^{-1} \quad \text{and} \quad \partial_cq = a^{-1} \otimes q. \quad (\text{A8})$$

Using this result, we then find that

$$\partial_{c^*}R = z(R \otimes 1)\partial_{c^*}q(1 \otimes R) = zRq \otimes (a^*)^{-1}R, \quad (\text{A9})$$

$$\partial_cR = z(R \otimes 1)\partial_cq(1 \otimes R) = zRa^{-1} \otimes qR. \quad (\text{A10})$$

Then, by the Leibniz rule,

$$\partial_{c^*}(qR) = (\partial_{c^*}q)(1 \otimes R) + (q \otimes 1)(\partial_{c^*}R) \quad (\text{A11})$$

$$= (q + zqRq) \otimes (a^*)^{-1}R \quad (\text{A12})$$

$$= qR \otimes (a^*)^{-1}R, \quad (\text{A13})$$

as $q + zqRq = qR$. Similarly, using the fact that q and R commute,

$$\partial_c(qR) = \partial_c(Rq) = Ra^{-1} \otimes qR. \quad (\text{A14})$$

Thus, using the integration by parts identities

$$\tau(cP) = g(\tau \otimes \tau)\partial_{c^*}P \quad (\text{A15})$$

$$\tau(c^*P) = g(\tau \otimes \tau)\partial_cP, \quad (\text{A16})$$

we have the two equations

$$\zeta M(z) - gM(z)\tau((a^*)^{-1}R) = \tau((a^*)^{-1}R), \quad (\text{A17})$$

$$\zeta^* M(z) - gM(z)\tau(a^{-1}R) = \tau(a^{-1}R), \quad (\text{A18})$$

or

$$\tau((a^*)^{-1}R) = \frac{\zeta M(z)}{1 + gM(z)} \quad (\text{A19})$$

$$\tau(a^{-1}R) = \frac{\zeta^* M(z)}{1 + gM(z)}. \quad (\text{A20})$$

To close these equations, we relate $\tau(a^{-1}R)$ and $\tau((a^*)^{-1}R)$ to $F(z)$ in another way. Starting from the defining property that $aa^{-1} = 1$, we expand the definition of a and trace against R to obtain

$$F(z) = \zeta\tau(a^{-1}R) - \tau(ca^{-1}R). \quad (\text{A21})$$

We now integrate by parts, using the fact that a^{-1} is a function only of c and thus has $\partial_{c^*} a^{-1} = 0$:

$$\tau(ca^{-1}R) = g(\tau \otimes \tau)(a^{-1} \otimes 1)\partial_{c^*} R \quad (\text{A22})$$

$$= gz(\tau \otimes \tau)(a^{-1}Rq \otimes (a^*)^{-1}R) \quad (\text{A23})$$

$$= gz\tau(a^{-1}Rq)\tau((a^*)^{-1}R) \quad (\text{A24})$$

$$= g[\tau(a^{-1}R) - \tau(a^{-1})]\tau((a^*)^{-1}R) \quad (\text{A25})$$

as $Rq = \frac{1}{z}(R - 1)$. Now, as ζ is outside the spectral radius of c ,

$$\tau(a^{-1}) = \tau((\zeta - c)^{-1}) = \frac{1}{\zeta}, \quad (\text{A26})$$

so we then find that

$$F(z) = \zeta\tau(a^{-1}R) - g \left[\tau(a^{-1}R) - \frac{1}{\zeta} \right] \tau((a^*)^{-1}R). \quad (\text{A27})$$

Substituting the expressions for $\tau(a^{-1}R)$ and $\tau((a^*)^{-1}R)$ that we found before into this equation and algebraically simplifying the result, this gives

$$F(z) = \frac{(|\zeta|^2 + g)M(z) + g^2M(z)^2}{(1 + gM(z))^2} \quad (\text{A28})$$

Recalling that $F(z) = 1 + zM(z)$, we can simplify this into a compact cubic equation for $M(z)$:

$$1 + gM(z) = |\zeta|^2 M(z) - zM(z)(1 + gM(z))^2. \quad (\text{A29})$$

We now want to use this to solve for the spectral density. To do so, we define $y = -gM(1/\lambda)$, and observe that the Stieltjes transform of the ζ -dependent spectral density is given by

$$G(s) = \frac{1}{s} - \frac{y(s)}{gs^2} \quad (\text{A30})$$

as $F(z) = 1 + zM(z)$ and $G(s) = F(1/s)/s$. Then, by Stieltjes inversion, the density is

$$\rho_\zeta(\lambda) = -\lim_{\epsilon \downarrow 0} \frac{1}{\pi g \lambda^2} \text{Im } y(\lambda - i\epsilon). \quad (\text{A31})$$

The cubic equation for $M(z)$ implies that y is a root of the cubic

$$y^3 - 2y^2 + (1 - (|\zeta|^2 - g)\lambda)y - g\lambda = 0. \quad (\text{A32})$$

This is a cubic with real coefficients, so a root with negative imaginary part exists when the discriminant

$$\lambda[4(|\zeta|^2 - g)^3\lambda^2 - (8|\zeta|^4 + 20|\zeta|^2g - g^2)\lambda + 4|\zeta|^2] \quad (\text{A33})$$

is negative. This is possible when $\lambda_- < \lambda < \lambda_+$, where

$$\lambda_{\pm} = \frac{2|\zeta|^4 + 5g|\zeta|^2 - \frac{1}{4}g^2 \pm \frac{1}{4}\sqrt{g}(8|\zeta|^2 + g)^{3/2}}{2(|\zeta|^2 - g)^3} \quad (\text{A34})$$

are the roots of the discriminant for $\lambda > 0$. Applying Cardano's formula, we find that in this regime

$$-\text{Im } y = \frac{3^{1/6}}{2} (\Delta_+^{1/3} - \Delta_-^{1/3}), \quad (\text{A35})$$

where

$$\begin{aligned} \Delta_{\pm} &= \left(|\zeta|^2 + \frac{g}{2} \right) \lambda - \frac{1}{9} \\ &\pm \sqrt{\frac{(|\zeta|^2 - g)^3 \lambda (\lambda - \lambda_-)(\lambda_+ - \lambda)}{3}}. \end{aligned} \quad (\text{A36})$$

We thus conclude at last that the density of eigenvalues of $\mathbf{Q}(\omega)$ is

$$\rho_\omega(\lambda) = \frac{3^{1/6}}{2\pi g \lambda^2} (\Delta_+^{1/3} - \Delta_-^{1/3}) \mathbf{1}_{\lambda_- < \lambda < \lambda_+}, \quad (\text{A37})$$

where we take real cube roots, and we must evaluate Δ_{\pm} at $|\zeta|^2 = 1 + \omega^2$.

Accounting for differences in notation, this is precisely the density found by Hu and Sompolinsky [2]. Hu and Sompolinsky [2] obtained this result using the replica trick; a recent paper from Tian *et al.* [8] used an alternative block-resolvent free probability approach to extend this result to the case in which $Q(\omega)$ is deformed by inserting a diagonal matrix of gains between the two resolvent factors.

Appendix B: Numerical methods

Here, we summarize the numerical methods used to generate the figures. The code used to generate Figures 1 and 2 was implemented in Python 3.10, using the NumPy and SciPy libraries [30]. The code used to generate Figure 3 was implemented in Matlab R2024b. All simulations—whether implemented in Python or Matlab—were run on a Dell Precision 7960 desktop workstation equipped with an Intel Xeon(R) w5-3525 processor and 128 GB of RAM.

To generate the theoretical predictions for the spectral density in Figure 1, we use an approximate numerical scheme to solve the functional equation (9) and evaluate

the inverse Stieltjes transform. To numerically approximate the solution to the functional equation, fix a point s at which we want to evaluate the Stieltjes transform $G(s) = F_d(1/s)/s$, and then set $z_0 = 1/s$. Define the iterates

$$z_{m+1} = gz_m F_d(z_m), \quad \text{so} \quad F_d(z_m) = \frac{1}{g} \frac{z_{m+1}}{z_m}. \quad (\text{B1})$$

Then, $F_d(z_{m+1}) = F_d(gz_m F_d(z_m))$. Using the functional equation $(1-z)F_d(z) = F_d(gzF_d(z))$, we thus find that

$$\frac{1}{g} \frac{z_{m+2}}{z_{m+1}} = F_d(z_m) = (1-z_m) \frac{1}{g} \frac{z_{m+1}}{z_m}. \quad (\text{B2})$$

Thus, z_m obeys the two-term recurrence

$$z_{m+2} = \frac{(1-z_m)z_{m+1}^2}{z_m}. \quad (\text{B3})$$

To fix a boundary condition, we use the fact that $F_d(z) \rightarrow 1$ as $z \rightarrow 0$, which allows us to solve backwards from z_M near zero for some large M to z_0 . This limiting behavior implies that

$$\frac{z_{m+1}}{z_m} \rightarrow g \quad (\text{B4})$$

as $m \rightarrow \infty$ if the sequence $z_m \rightarrow 0$. Thus, we set some large cutoff M (in our simulations we find that $M = 75$ is large enough to obtain a good match to experiments, though we have not made an effort to optimize this), and set $z_M = \alpha g^M$ and $z_{M+1} = \alpha g^{M+1}$ for some amplitude α . Then, we run the recurrence backwards from $m = M$ to $m = 0$ using the expression

$$z_m = \frac{z_{m+1}^2}{z_{m+1}^2 + z_{m+2}}, \quad (\text{B5})$$

and then fix α by matching the initial condition $z_0 = 1/s$.

Given this approximate solution, we then recover the Stieltjes transform by using the fact that

$$G(s) = \frac{1}{s} F_d\left(\frac{1}{s}\right) = z_0 F_d(z_0) = \frac{1}{g} z_1. \quad (\text{B6})$$

To estimate the spectral density at the point λ , we set $s = \lambda - i\epsilon$ for some fixed value of ϵ , solve for z_1 at each point, and then take $\text{Im} z_1 / \pi g$ as our estimate of the density. We choose ϵ large enough such that the iteration is stable even as $\text{Re}(z_m)$ enters the spectral support; in practice we take $\epsilon = 0.06$.

We use the same iterative scheme to approximately solve for the upper spectral edge λ_+ . Instead of enforcing $z_0 = 1/s$, we instead maximize $z_0(\alpha)$ with respect to α using `scipy.optimize.minimize_scalar`, and then estimate $\lambda_+ = 1/\max_{\alpha>0} z_0(\alpha)$. This gives us a rough estimate of the location where the branch of F_d outside the support ceases to become locally invertible.

To obtain a more quantitative comparison between the empirical and predicted spectral distributions, in Figure 3 we consider the first eight moments across varying

values of g . To produce the theoretical predictions, we solve the moment recurrence (12) by hand for the first few orders, and then using SymPy up to $n = 8$. The expressions for the moments are rational functions of g whose precise forms are not illuminating; we therefore do not list them here, and direct the reader to the GitHub for the SymPy code. These predictions are then passed into a Matlab script which compares them against the result of numerically estimating the spectral moments across a range of values of g ; this forms the basis for Figure 3. We restrict our attention to $g \leq 0.8$ as the theory predicts that $m_8(g = 0.8)$ is on the order of 10^{11} ; larger values and higher moments are even larger, and numerical stability becomes an issue. Moreover, high-order moments at large g are dominated by rare large eigenvalues.

This is therefore a fully independent numerical check, as it relies on a different method for computing the empirical spectrum than the Python code used elsewhere. Here, as in Figure 2, we enforce a stability threshold on each realization of \mathbf{J} so that the computation of Σ_d is numerically stable. Concretely, in code we generate new realizations of \mathbf{J} until the condition $\rho(\mathbf{J}) < 1 - \epsilon$ is satisfied, for a stability threshold $\epsilon = 10^{-3}$. In practice, we found that one attempt was sufficient for all of the realizations at $N = 4096$ used in Figure 3. There, we show the log-ratio $\log_{10}(\hat{m}_n/m_n^{th})$ between the measured and predicted moments across g ; from this we see that the ratiometric error is at most around $10^{0.15} \simeq 1.035$ for $g = 0.8$, where the raw value of the moment is around 10^{11} .

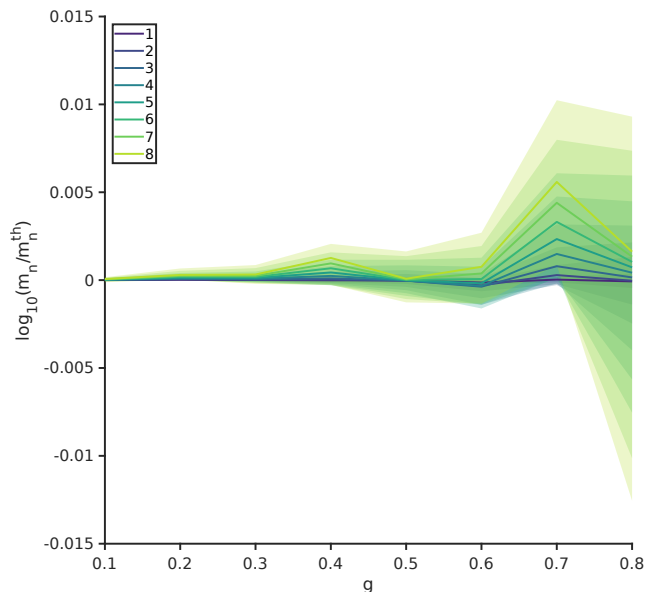


FIG. 3. Comparison of empirical and predicted spectral moments across gains g . Empirical moments are estimated based on 25 realizations at $N = 4096$. Shaded patches show 95% confidence intervals on the log-relative-error $\log_{10}(\hat{m}_n/m_n^{th})$ estimated using bootstrapping.

- [1] H. Sompolinsky, A. Crisanti, and H. J. Sommers, Chaos in random neural networks, *Physical Review Letters* **61**, 259 (1988).
- [2] Y. Hu and H. Sompolinsky, The spectrum of covariance matrices of randomly connected recurrent neuronal networks with linear dynamics, *PLOS Computational Biology* **18**, 1 (2022).
- [3] G. Hennequin, T. P. Vogels, and W. Gerstner, Non-normal amplification in random balanced neuronal networks, *Physical Review E* **86**, 011909 (2012).
- [4] T. Toyozumi and L. F. Abbott, Beyond the edge of chaos: Amplification and temporal integration by recurrent networks in the chaotic regime, *Physical Review E* **84**, 051908 (2011).
- [5] F. Mastrogiuseppe, J. Carmona, and C. K. Machens, Stochastic activity in low-rank recurrent neural networks, *PLOS Computational Biology* **21**, 1 (2025).
- [6] B. Bordelon, J. Cotler, C. Pehlevan, and J. A. Zavatone-Veth, Dynamics of learning to integrate in linear recurrent neural networks, *arXiv* (2026).
- [7] J. T. Chalker and B. Mehlige, Eigenvector statistics in non-Hermitian random matrix ensembles, *Physical Review Letters* **81**, 3367 (1998).
- [8] G. J. Tian, O. Zhu, V. Shirhatti, C. M. Greenspon, J. E. Downey, D. J. Freedman, and B. Doiron, Firing rate diversity lowers the dimension of population covariability in neuronal networks, *bioRxiv* 10.1101/2024.08.30.610535 (2026).
- [9] R. Couillet, G. Wainrib, H. T. Ali, and H. Sevi, A random matrix approach to echo-state neural networks, in *Proceedings of The 33rd International Conference on Machine Learning*, Proceedings of Machine Learning Research, Vol. 48, edited by M. F. Balcan and K. Q. Weinberger (PMLR, New York, New York, USA, 2016) pp. 517–525.
- [10] C. W. Gardiner, *Handbook of stochastic methods*, Vol. 3 (Springer Berlin, 1985).
- [11] M. Pachitariu, L. Zhong, A. Gracias, A. Minisi, C. Lopez, and C. Stringer, A critical initialization for biological neural networks, *Nature* 10.1038/s41586-026-10528-1 (2026).
- [12] X. Chen and W. Bialek, Searching for long timescales without fine tuning, *Physical Review E* **110**, 034407 (2024).
- [13] C. Stringer, M. Pachitariu, N. Steinmetz, M. Carandini, and K. D. Harris, High-dimensional geometry of population responses in visual cortex, *Nature* **571**, 361 (2019).
- [14] V. M. Preciado and M. A. Rahimian, Controllability Gramian spectra of random networks, in *2016 American Control Conference (ACC)* (2016) pp. 3874–3879.
- [15] C. Godrèche and J.-M. Luck, Characterising the nonequilibrium stationary states of Ornstein–Uhlenbeck processes, *Journal of Physics A: Mathematical and Theoretical* **52**, 035002 (2018).
- [16] Y. V. Fyodorov, E. Gudowska-Nowak, M. A. Nowak, and W. Tarnowski, Nonorthogonal eigenvectors, fluctuation-dissipation relations, and entropy production, *Physical Review Letters* **134**, 087102 (2025).
- [17] L. S. Ferreira, F. L. Metz, and P. Barucca, Random matrix ensemble for the covariance matrix of Ornstein-Uhlenbeck processes with heterogeneous temperatures, *Physical Review E* **111**, 014151 (2025).
- [18] X. Shen and Y. Hu, Covariance spectrum in nonlinear recurrent neural networks, *arXiv* (2025).
- [19] J. A. Mingo and R. Speicher, *Free Probability and Random Matrices* (Springer New York, New York, NY, 2017).
- [20] A. Guionnet, Free analysis and random matrices, *Japanese Journal of Mathematics* **11**, 33 (2016).
- [21] S.-S. Byun and P. J. Forrester, Progress on the study of the Ginibre ensembles II: GinOE and GinSE, *arXiv* (2023).
- [22] B. Collins, T. Mai, A. Miyagawa, F. Parraud, and S. Yin, Convergence for noncommutative rational functions evaluated in random matrices, *Mathematische Annalen* **388**, 543 (2024).
- [23] D. Martí, N. Brunel, and S. Ostojic, Correlations between synapses in pairs of neurons slow down dynamics in randomly connected neural networks, *Physical Review E* **97**, 062314 (2018).
- [24] S. Belinschi, B. Kołodziejek, and K. Szpojankowski, Free perpetuities I: Existence, subordination and tail asymptotics, *arXiv* (2025).
- [25] B. Kołodziejek and K. Szpojankowski, On the empirical spectral distribution of matrix perpetuities, *arXiv* (2026).
- [26] D. G. Clark, Linear equivalence of nonlinear recurrent neural networks, *arXiv* (2026).
- [27] A. J. Wakhloo, Solution of a large nonlinear recurrent neural network at fixed connectivity, *arXiv* (2026).
- [28] Y. M. Lu and H.-T. Yau, An equivalence principle for the spectrum of random inner-product kernel matrices with polynomial scalings, *The Annals of Applied Probability* **35**, 2411 (2025).
- [29] A. Atanasov, J. A. Zavatone-Veth, and C. Pehlevan, Scaling and renormalization in high-dimensional regression, *Journal of Statistical Mechanics: Theory and Experiment* **2026**, 043404 (2026).
- [30] P. Virtanen, R. Gommers, T. E. Oliphant, M. Haberland, T. Reddy, D. Cournapeau, E. Burovski, P. Peterson, W. Weckesser, J. Bright, S. J. van der Walt, M. Brett, J. Wilson, K. J. Millman, N. Mayorov, A. R. J. Nelson, E. Jones, R. Kern, E. Larson, C. J. Carey, Í. Polat, Y. Feng, E. W. Moore, J. VanderPlas, D. Laxalde, J. Perktold, R. Cimrman, I. Henriksen, E. A. Quintero, C. R. Harris, A. M. Archibald, A. H. Ribeiro, F. Pedregosa, P. van Mulbregt, and SciPy 1.0 Contributors, SciPy 1.0: Fundamental Algorithms for Scientific Computing in Python, *Nature Methods* **17**, 261 (2020).